Vol 18 No 4, April 2009
1674-1056/2009/18(04)/1491-07

Chinese Physics B

© 2009 Chin. Phys. Soc.
and IOP Publishing Ltd

# An *ab initio* study of niobium ($n$ = 2–11) clusters: structure, stability and magnetism*

Ren Feng-Zhu(任凤竹)†, Wang Yuan-Xu(王渊旭), Zhang Guang-Biao(张光彪), Wei Shu-Ke(魏书克), and Luo You-Hua(罗有华)

*Institute of Computational Materials Science, School of Physics and Electronics, Henan University, Kaifeng* 475004, *China*

(Received 4 March 2008; revised manuscript received 29 July 2008)

The ground-state configurations of the $Nb_n$ ($n$ = 2–11) clusters are studied through the first-principles calculations. It is found that niobium clusters ($n$ = 2–11) tend to form compact structures with low symmetry. The clusters with 4, 8 and 10 atoms are found to be magic and have relatively large highest occupied–lowest unoccupied molecular orbital (HOMO-LUMO) gaps. The $Nb_n$ clusters possess low magnetic moments, which exhibit an odd-even oscillational character. The analyses of calculated electronic density and population of the lowest-energy niobium clusters for $n$ = 2, 3, 5, 7, 9, 11 show that the total magnetic moments of $Nb_n$ originate mainly from a few Nb atoms with longer spacings between them in most cases, while they are located on two Nb atoms for $n$ = 2, 3, 5. The total magnetic moments come mainly from the 4*d* local moments but with the exception of the $Nb_5$ cluster.

**Keywords:** $Nb_n$ cluster, density functional theory, structure, stability and magnetism
**PACC:** 3640, 3640B, 7115M

## 1. Introduction

In recent years, many transition metal clusters have been studied both experimentally and theoretically for their fundamental importance and potential applications as magnetic material and chemical catalysis. Niobium cluster is one of the most extensively investigated transition-metal clusters due to their several features, such as the relatively great propensity to form clusters and the appearance of ferroelectric state related to superconductivity.[1−13] Small niobium clusters have been well studied by using various experimental methods.[3,5,6,9,12] Photoemission determination of niobium clusters suggested large highest occupied-lowest unoccupied molecular orbital (HOMO-LUMO) gaps for 8, 10, 16 atom clusters.[12] Mass spectrum of autoionized niobium clusters showed marked intensities for $n$ = 7, 13, 15, 22 with magic behaviour and a minimum in the abundance (intensity) for $n$ = 19.[5]

The structural features and the electronic properties of niobium clusters have been theoretically investigated through different approaches by several groups, such as Kumar and Kawazoe,[1] Grönbeck *et al*,[7] and Goodwin and Salahub.[10] However, their results are different. Therefore it is necessary to study niobium clusters by using an accurate method. The most interesting property of niobium clusters is nonmagnetic in bulk but the experiment shows that the magnetic moments in niobium clusters change nonmonotonically with cluster size. In the present study, the geometry optimizations and properties of the $Nb_n$ ($n$ = 2–11) clusters are investigated by using the density-functional theory with the unrestricted B3LYP exchange-correlation potential[14,15]and an effective core potential LanL2DZ basis sets.[16] The standard LanL2DZ basis sets provides an effective way to reduce difficulties in calculating two-electron integrals caused by heavy transition-metal atoms. On the other hand, ($n$-1)*s*, ($n$-1)*p*, ($n$-1)*d*, *ns* and *np* orbitals are taken as valence electron orbitals in the LanL2DZ basis sets which can obviously enhance the calculation accuracy. Moreover, we investigate the magnetic properties of $Nb_n$ ($n$ = 2–11) clusters and the calculated results are compared with the experimental results.

*Project supported by the Program for Science & Technology Innovation Talents in Universities of Henan Province, China (Grant No 2009HASTIT003), the Natural Science Foundation of Henan University, China (Grant Nos 07ZRZD005 and 07YBZR046), and the Foundation of Science and Technology Department of Henan Province, China (Grant No 082300410010).
†Corresponding author. E-mail: f.z.ren@henu.edu.cn

## 2. Computational methods

In order to determine exchange-correlation potential, the $Nb_2$ is calculated with B3LYP, B3PW91, HCHT, MPW1PW91, PBEPBE, PBE1PBE and the results are listed in Table 1. The theoretical results with B3LYP indicate that the triplet $Nb_2$ is the most stable state, and that the Nb-Nb bond length is 0.212 nm with an average binding energy of 2.59 eV, which is in excellent agreement with the experimental values of 0.208 nm and 2.60 eV, separately.[2,9] Consequently, B3LYP is proved to be applicable for the $Nb_n$ clusters. All theoretical calculations above were performed with GAUSSIAN-03 package.[17] The previous studies on the niobium clusters,[1,4,7,8,10,11] and on others transition-metal (TM) clusters such as zirconium, gold, cobalt, nickel, ruthenium, rhodium, palladium, osmium, platinum, iridium and tantalum clusters were seen as a guide to considering $Nb_n$ geometries. In the present paper, equilibrium geometries of the $Nb_n$ clusters are optimized, and their stabilities are reassured accurately by the harmonic vibrational frequency calculations. In order to further explore the origins of the magnetic moments, we also calculate the electron density and perform the population analysis of the clusters with Dmol$^3$ package.[18]

**Table 1.** Measured and calculated results of bond length $R$ (in nm), average binding energy $E_b$ (in eV), vibrational frequency $\omega$ (in $cm^{-1}$) for $Nb_2$ by using B3LYP, B3PW91, HCHT, MPW1PW91, PBEPBE and PBE1PBE.

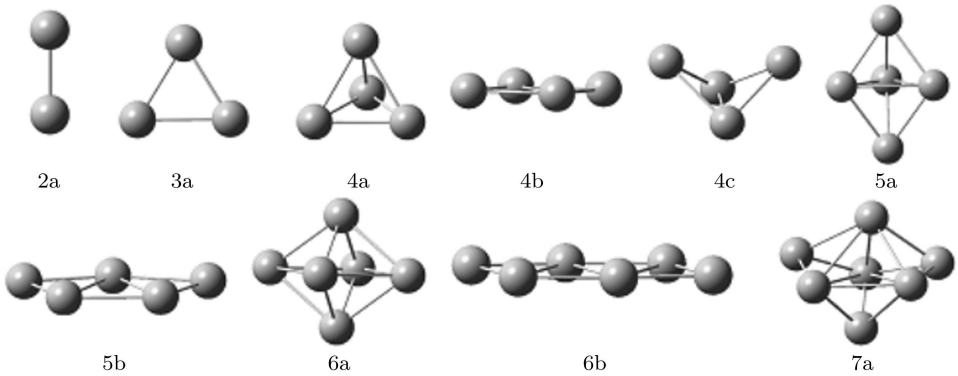
| | B3LYP | B3PW91 | HCHT | MPW1PW91 | PBEPBE | PBE1PBE | Experiment |
|---|---|---|---|---|---|---|---|
| $R$ | 0.212 | 0.210 | 0.212 | 0.212 | 0.214 | 0.212 | 0.208[a] |
| $E_b$ | 2.59 | 3.38 | 4.05 | 3.26 | 3.29 | 3.39 | 2.60[b] |
| $\omega$ | 427.34 | 480.15 | 464.15 | 485.91 | 456.79 | 485.82 | 424.89[c] |

[a]from Ref.[2].
[b]from Ref.[9].

## 3. Results and discussion

### 3.1. Equilibrium geometries

The lowest-energy structures as well as the metastable configurations of the $Nb_n$ ($n = 2$–11) clusters are presented in Fig.1 and described in Table 2 where their geometries, symmetries, average distances of the ground state, average atomic coordination numbers and relative energies from the ground state are displayed. According to their energy ordering, the isomers are labelled as *na*, *nb*, *nc*, and so on, where *na* is corresponding to the lowest-energy isomer. Since the spacings between the nearest-neighbouring atoms in the $Nb_n$ clusters are different, we define the average distance $\bar{R}$ as $\bar{R} = \frac{1}{N_b} \sum_{i,j,i\neq j} R_{ij}$, where $R_{ij}$ is the nearest-neighbouring spacing, which is 15% less than the minimal spacing between $i$ and $j$ atoms, $N_b$ is the number of bonds in the cluster. The average atomic coordination number is the average number of the nearest neighbours and defined as $N_C = \frac{1}{n}\sum_i n_i$, where $n$ is the number of atoms in the Nb cluster, and $n_i$ is the number of the nearest-neighbouring atoms for the $i$-th atom in the cluster.



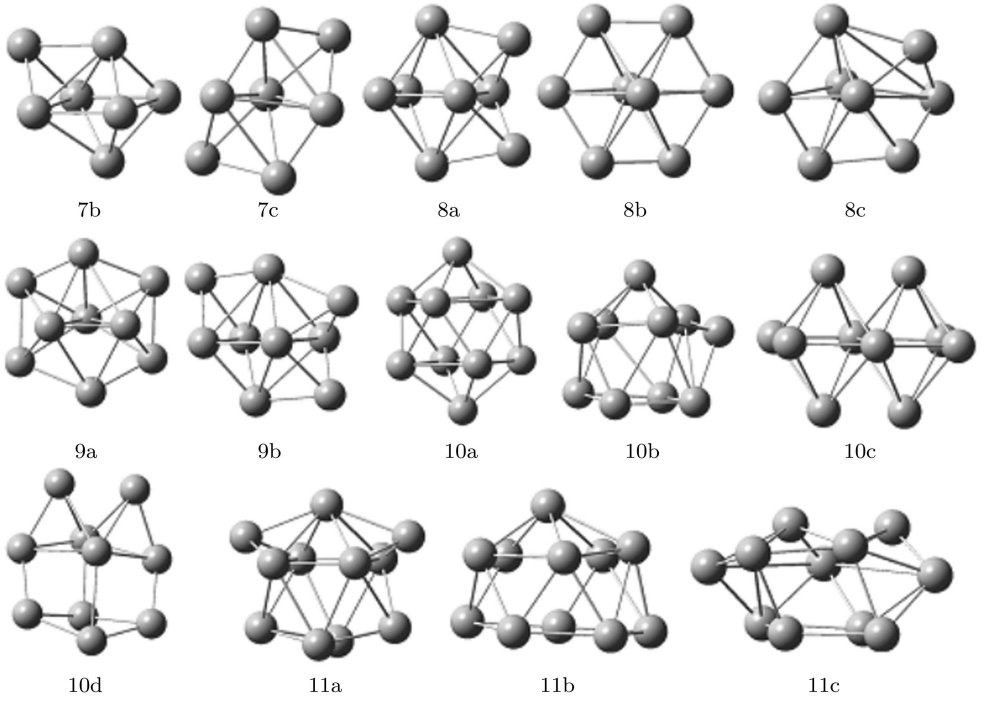



**Fig.1.** Calculated lowest-energy and low-lying structures of $Nb_n$ ($n$ = 2–11) clusters.

**Table 2.** Geometry, symmetry (Sym in short), average spacing $\bar{R}$ (in nm) of the ground state, average atomic coordination number $N_C$ and energy difference $\Delta E$ (in eV) between equilibrium geometries and the ground state of $Nb_n$ clusters.

| $n$ | geometry | Sym | $\bar{R}$ | $N_c$ | $\Delta E$ |
|---|---|---|---|---|---|
| 2 | linear (2a) | $D_{\infty h}$ | 0.212 | 1 | 0 |
| 3 | triangle (3a) | $C_s$ | 0.231 | 2 | 0 |
| | linear (3b) | $D_{\infty h}$ | | 1.33 | 4.219 |
| 4 | pyramidal (4a) | $C_3$ | 0.254 | 3 | 0 |
| | rhombus (4b) | $D_{2h}$ | | 2 | 0.961 |
| | bendrhombus (4c) | $C_{2v}$ | | 2.5 | 1.476 |
| 5 | distorted trigonal bipyramid (5a) | $C_{2v}$ | 0.258 | 3.2 | 0 |
| | planar W (5b) | $C_s$ | | 1 | 1.791 |
| 6 | tetragonal bipyramid (6a) | $D_{2h}$ | 0.255 | 3 | 0 |
| | a planar structure (6b) | $C_{2h}$ | | 1.33 | 0.353 |
| 7 | bicapped trigonal bipyramid (7a) | $C_1$ | 0.263 | 3.14 | 0 |
| | capped tetragonal bipyramid (7b) | $C_s$ | | 3.14 | 0.701 |
| | bicapped trigonal bipyramid (7c) | $C_2$ | | 2.86 | 1.331 |
| 8 | capped octahedron (8a) | $D_2$ | 0.258 | 3 | 0 |
| | capped octahedron in skewed (8b) | $C_1$ | | 3.25 | 0.628 |
| | capped octahedron in trans (8c) | $C_2$ | | 3.25 | 0.866 |
| 9 | twinborn bioctahedron (9a) | $C_2$ | 0.252 | 2.44 | 0 |
| | Capped tetragonal (9b) | $C_s$ | | 2.89 | 0.588 |
| 10 | bicapped antiprism (10a) | $C_4$ | 0.258 | 3.3 | 0 |
| | distorted bicapped antiprism (10b) | $C_3$ | | 3.1 | 0.64 |
| | twinborn bioctahedron (10c) | $D_{2h}$ | | 2.4 | 0.98 |
| | tricapped pentagonal bipyramid (10d) | $C_s$ | | 2.82 | 1.01 |
| 11 | capped antiprism (11a) | $C_{2v}$ | 0.260 | 3.4 | 0 |
| | distorted capped antiprism (11b) | $C_2$ | | 3.8 | 0.64 |
| | bicapped antiprism (11c) | $C_1$ | | 3.8 | 0.66 |

The equilibrium geometries obtained in the present study are in accord with those in the previous studies in most cases.[1,4,10,11] $Nb_3$ is a nearly equilateral triangle of spin multiplicity 2 with sides of 0.236, 0.237, and 0.234 nm. These are in accord with those in a nearly equilateral triangle geometry with $D_{3h}$ symmetry obtained by spectroscopy of mass-selected Nb clusters,[6] though they are different from those for an isosceles triangle obtained by Kumar and Kawazoe.[1] Frequency analysis shows that a planar W-type structure with $C_s$ symmetry (in Fig.1(5b)) is a transition state. We tried to superimpose $C_s$ structure onto $C_{2v}$ structure and to optimize it, but the result shows that the $C_{2v}$ structure is also of a transition state. Frequency analysis also shows that a planar structure with $C_{2h}$ symmetry (in Fig.1(6b)) is of a transition state. For $Nb_9$, the ground state can be viewed as a state of distorted twinborn bioctahedron structure with $C_2$ symmetry, and this structure is similar to the metastable one obtained from Ref.[1]. Another structure (in Fig.1(9b)) can be considered as a structure of sightly distorted capped tetragonal prism. The structure shown in Fig.1(9b) is 0.57 eV higher in energy than the ground state indicated in Fig.1(9a). For $Nb_{10}$, the lowest energy structure is of a bicapped antiprism (in Fig.1(10a)), which could be considered to arise from the capping of a prism. Another two structures in Figs.1(10b) and 1(10c) can be regarded as twinborn bioctahedron and tricapped tetragonal bipyramids with $D_{2h}$, and $C_s$ symmetries, respectively. The lowest-energy structure of $Nb_{11}$ in Fig.1(11a) can be obtained by capping one atom on the top of tetragonal prism which is different from the two pentagonal bipyramids fused at a triangular face.[1] Similarly, the metastable isomers in Figs.1(11b) and 1(11c) can be obtained by capping one atom on the face or edge of the pentagonal prism, and they are 0.64 and 0.65 eV higher in energy than the ground state respectively. Figure 1 and Table 2 indicate that the small Nb clusters tend to form the compact structures with low symmetry based on either a tetrahedron or a prism of the larger average coordination number.

## 3.2. Relative stability

In order to analyse the stability and the size-dependent physical properties of the Nb clusters, we calculate the binding energy per atom, $E_b$, which is defined as

$$E_{\mathrm{b}} = [nE_1 - E_n]/n, \tag{1}$$

where $E_1$ and $E_n$ represent the energy of one Nb atom before $n$ Nb atoms are bound into an $Nb_n$ cluster and the lowest energy of the $Nb_n$ cluster structure, respectively. The $E_{\mathrm{b}}$ value of the lowest-energy $Nb_n$ cluster is displayed in Fig.2. As seen in this figure, the binding energy increases monotonically as the size of clusters increases. Thus, the clusters can continue to gain

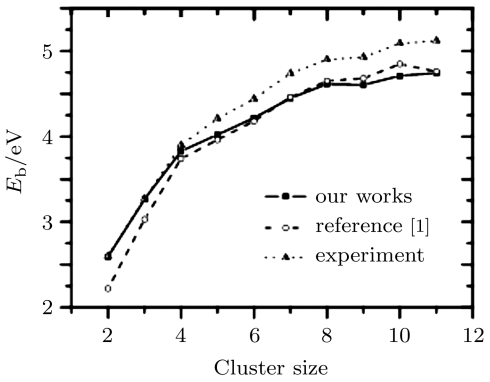



**Fig.2.** Measured and calculated results of binding energy per atom $E_{\mathrm{b}}$ of the lowest-energy $Nb_n$ ($n = 2$–11) clusters.

energy during the growth, therefore this system may form a greater size cluster. It also suggests that the energy convergence to bulk behaviour is slow in these small clusters in which the surface effect may be important. Furthermore, the results show that the method selected in the present work is more accurate for small clusters ($n \leq 7$). In cluster physics, the second-order difference in energy is a sensitive quantity that reflects the relative stability of investigated clusters. The second-order difference in energy is $\Delta_2 E(n)$, which is defined as

$$\Delta_2 E(n) = E(n+1) + E(n-1) - 2E(n), \tag{2}$$

where $E(n)$, $E(n-1)$, and $E(n+1)$ represent the total energies of the lowest energy structure $Nb_n$, $Nb_{n-1}$, and $Nb_{n+1}$ clusters, respectively. As shown in Fig.3, the values of magic number of Nb cluster, $n$, are found to be 4, 8 and 10, implying that these clusters are more stable than their neighbouring clusters. According to Fig.3, the value of $\Delta_2 E$ has an evident peak for $n = 10$, namely $Nb_{10}$ cluster is the most stable.

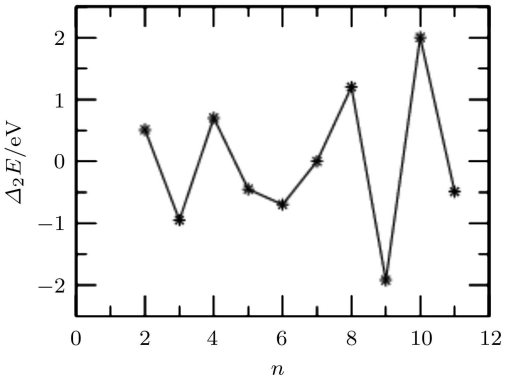



**Fig.3.** Calculated results of second-order difference in energy $\Delta_2 E$ of the lowest-energy $Nb_n$ ($n$ = 2–11) clusters.

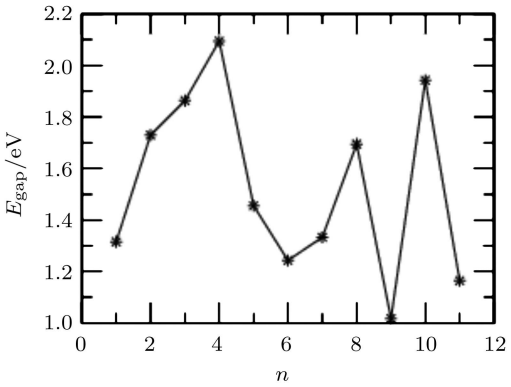



**Fig.4.** Calculated values of HOMO-LUMO gap $E_{gap}$ of the lowest-energy $Nb_n$ ($n$ = 2–11) clusters.

## 3.3. Electronic properties

The HOMO-LUMO gap ($E_{gap}$) is considered to be an important parameter to estimate the electronic stability of small clusters. According to the Koopmanns theory, the HOMO energy level reflects the cluster ability during losing its electrons, the higher HOMO energy level means losing the electrons more easily. While the LUMO energy level is equal to the electron affinity potential in value, the lower LUMO energy level indicates that it is easier for the cluster to obtain the electrons. The $E_{gap}$ reflects the ability for electrons to jump from occupied orbital to unoccupied orbital and represents the ability for the molecular participates to produce chemical reactions to some degree. A large $E_{gap}$ corresponds to a high strength required to perturb the electronic structure, namely a bigger $E_{gap}$ indicates a weaker chemical activity. The $E_{gap}$ as a function of number of Nb atoms, $n$, is shown in Fig.4, it is seen that the gap of the $Nb_n$ clusters oscillates significantly as a function of number of Nb atoms. Remarkable peaks appear at sizes of $n$ = 4, 8, 10, suggesting that these clusters are more stable than their neighbouring clusters, which accords with the behaviour of the second-order energy difference $\Delta_2 E$ (Fig.4). The change role of the $E_{gap}$ in the present study is similar to that presented in Ref.[1] except the case for $n$ = 6. In light of the particular phenomenon where the gap of $Nb_4$ cluster is the largest but the gap of $Nb_9$ is the smallest in niobium clusters ($n$ = 2–11), the energy levels of molecular orbital for Nb, $Nb_4$ and $Nb_9$ are displayed in Fig.5. Compared with Nb and $Nb_9$, $Nb_4$ obviously is characteristic of the molecular orbital producing the degeneration of the energy level in the vicinity of the HOMO-LUMO and the energy level of the LUMO elevated strongly, which probably leads to its largest value of $E_{gap}$.

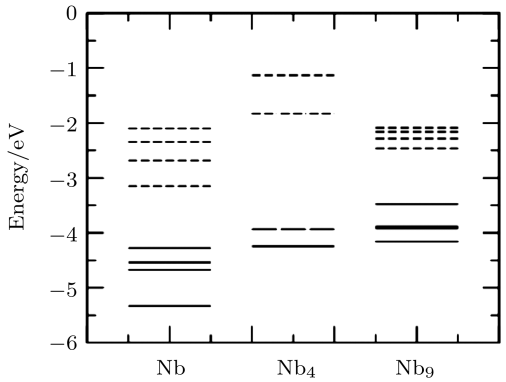



**Fig.5.** Energy levels of one electron in the vicinity of the HOMO and LUMO of Nb, $Nb_4$ and $Nb_9$.

## 3.4. Magnetic moments

As mentioned in the introduction, i.e. in Section 1, the most interesting property of niobium clusters is nonmagnetic in bulk but the experiment shows that the magnetic moments in niobium clusters change nonmonotonically with cluster size. Detailed data on the magnetic behaviour of niobium clusters in a size range of 3–52 atoms have recently become available from molecular beam Stern–Gerlach deflection experiment[3] at $T$ = 20 K. In Fig.6, our theoretical results reproduce basically the same tendency of experimental $\mu_n$ within experimental accuracy except for that of $Nb_7$ cluster. The deviation of the theoretical result from the experimental result, which happens to $Nb_7$ cluster, can be attributed to the existence of energetically closely lying isomer ($\Delta E$ = 0.701 eV) of $C_s$ symmetry. The calculated total magnetic moment of 0.806 $\mu_B$ for $C_s$ isomer is in good agreement with the measured one. The odd-$n$ clusters each have a magnetic moment, i.e. $\mu_n = 1\mu_B$, which is consistent with the magnetic moment of a single unpaired electron. Even-$n$ clusters each possess $\mu_n = 0$ (except even 2-cluster that has $\mu_2 = 2\mu_B$). It is interesting to note

that the magnetic moments of $Nb_n$ ($n$ = 2–11) clusters exhibit an odd-even oscillational character. The odd number of valence electrons in an atom of the clusters can lead to a significant even-odd alternation in cluster properties, which can explain the tendency of behaviour in magnetic moment for $Nb_n$ ($n$ = 2–11) clusters.

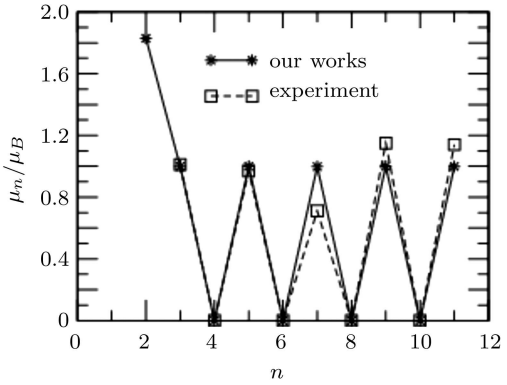



**Fig.6.** Values of total magnetic moment $\mu_n$ of the lowest-energy $Nb_n$ ($n$ = 2–11) clusters.

It is well known that the magnetic behaviour is very sensitive to the details of local atomic environment, e.g. symmetry, coordination number, interatomic spacing, and electronic density distribution. In general, the higher symmetry, smaller coordination number and longer interatomic spacing are accompanied with the larger magnetic moments as these factors tend to reduce electron overlap. In order to further understand the magnetic moment, the analyses of the electron density and the electron population of the lowest-energy niobium clusters for $n$ = 2, 3, 5, 7, 9, 11 are calculated and illustrated in Fig.7 and Table 3. From Fig.7, one can see that the total magnetic moments of the clusters originate from a small number of Nb atoms in most cases. However, they are located on two Nb atoms for $Nb_2$, $Nb_3$ and $Nb_5$. We also analyse the spacing between the Nb atoms. The results indicate that the contribution of the Nb atoms with longer spacings between them to the magnetic moment is great. A different bond length between the Nb atoms would naturally cause an obvious distinction of mutual interaction between them. A longer interspace generally suggests a weaker interaction between the Nb atoms, which will result in the production of more unpaired electrons in them. Consequently, their contribution to the magnetic moment is great. On the contrary, there is little contribution to the magnetic moment, made by the Nb atoms with shorter interspaces because their strong interaction may reduce the number of the unpaired electrons.

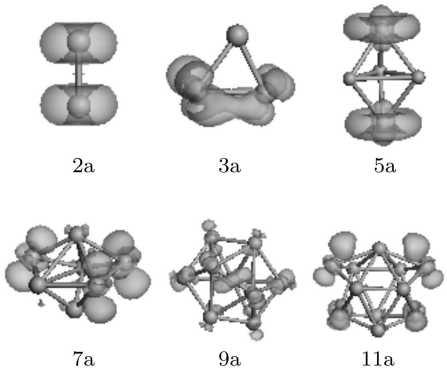



**Fig.7.** Differences in charge density between up-spin and down-spin electrons of the lowest-energy $Nb_n$ clusters for $n$ = 2, 3, 5, 7, 9, 11.

**Table 3.** The values of total moment $\mu_n$ and local spin magnetic moments $\mu_{4s}, \mu_{4p}, \mu_{4d}, \mu_{5s}$ and $\mu_{5p}$ of the lowest-energy niobium clusters for $n$ = 2, 3, 5, 7, 9 , 11.

| $n$ | $\mu_n/\mu_B$ | $\mu_{4s}/\mu_B$ | $\mu_{4p}/\mu_B$ | $\mu_{4d}/\mu_B$ | $\mu_{5s}/\mu_B$ | $\mu_{5p}/u_B$ |
|---|---|---|---|---|---|---|
| 2 | 1.829 | –0.002 | 0.014 | 1.480 | 0.336 | –0.002 |
| 3 | 0.999 | 0.002 | 0.010 | 0.986 | –0.01 | 0.009 |
| 5 | 1.000 | 0.002 | 0.005 | 0.158 | 0.674 | 0.161 |
| 7 | 0.988 | 0 | 0.006 | 0.541 | 0.357 | 0.093 |
| 9 | 1.000 | 0.001 | 0.007 | 0.626 | 0.305 | 0.059 |
| 11 | 0.988 | 0 | 0.009 | 0.609 | 0.273 | 0.109 |

So different magnetic behaviours of $Nb_2$ ($D_{\infty h}$), $Nb_3$ ($C_s$) and $Nb_5$ ($C_{2v}$) may be due to the joint-effect originating from different kinds of factors. The charge transfer between non-equivalent atoms and *spd* orbitals of an atom plays an important role in the distribution of local spin magnetic moment. The local charge neutrality used in the present study basically prohibits the charge transfer between non-equivalent atoms but permits it

to take place between orbitals of an atom. From Table 3, one can easily see that the electrons of the 5$s$ are redistributed to the 4$d$ and the 5$p$ orbitals. The cluster magnetic moments come mainly from the 4$d$ local moments, while the local moments of the 5$s$ and 5$p$ orbitals are much smaller than $\mu_{4d}$ (except $n = 5$).

## 4. Conclusions

First-principles calculation is performed to study geometric structures, relative stabilities, electronic properties, and magnetic moments of $Nb_n$ ($n$ = 2–11) clusters. Small $Nb_n$ clusters ($n \leq 11$) tend to form compact structures with low symmetry based on either a tetrahedron or a prism of larger average coordination number. The magnetic moments of ground states $Nb_n$ ($n$ = 2–11) clusters exhibit an odd-even oscillational character. The analyses of the calculated electronic density and population of the lowest-energy niobium clusters for $n$ = 2, 3, 5, 7, 9, 11 show that the total magnetic moments of $Nb_n$ originate mainly from a few Nb atoms with longer spacings between them in most cases, while they are located on two Nb atoms for $Nb_2$, $Nb_3$ and $Nb_5$. The charge transfers among *spd* orbitals of an atom lead to the fact that the total magnetic moments come mainly from the 4$d$ local moments but with the exception of the $Nb_5$ cluster. The results indicate that there are large HOMO-LUMO gaps for 4, 8, 10 atoms and clusters are found to be magic, however, with the exception of the $Nb_6$ cluster. The calculated binding energies and magnetic moments are in good agreement with experimental data and provide a support for the theoretical results of the structures presented in the present study and an insight into more complicated cluster systems.

## References


[1] Kumar V and Kawazoe Y 2002 *Phys. Rev.* B **65** 125403
[2] Hales D A, Lian L and Armentrout P B 1990 *Int. J. Mass Spectrom. Ion Processes* **102** 269
[3] Moro R, Yin S Y, Xu X S and de Heer Walt A 2004 *Phys. Rev. Lett.* **93** 086803
[4] Majumdar D and Balasubramaniana K 2004 *J. Chem. Phys.* **121** 4014
[5] Sakurai M, Watanabe K, Sumiyama K and Suzuki K 1999 *J. Chem. Phys.* **111** 235
[6] Wang H M, Craig R, Haouari H, Liu Y F, Lombardi J R and Lindsay D M 1996 *J. Chem. Phys.* **105** 5355
[7] Grönbeck H, Rosen A and Andreoni W 1998 *Phys. Rev.* A **58** 4630
[8] Fournier R, Pang T and Chen C F 1998 *Phys. Rev.* A **57** 3683
[9] James A M, Kowalczyk P, Fournier R and Simard B 1993 *J. Chem. Phys.* **99** 8504
[10] Goodwin L and Salahub D R 1993 *Phys. Rev.* A **47** R774
[11] Folwler J E, Garcia A and Ugalde J M 1999 *Phys. Rev.* A **60** 3058
[12] Kietzmann H, Morenzin J, Bechthold P S, Gantefor G and Eberhardt W 1998 *J. Chem. Phys.* **109** 2275
[13] Wei F, Luo C F and Dong J M 2005 *Phys. Rev.* B **71** 245415
[14] Becke A D 1988 *Phys. Rev.* A **38** 3098
[15] Lee C, Yang W and Parr R G 1988 *Phys. Rev.* B **27** 785
[16] Hay P J and Wadt W R 1985 *J. Chem. Phys.* **82** 270
[17] Frish M J, Trucks G W, Schlegel H B *et al* 2003 GAUSSIAN 03, Gaussian, Inc., Pittsburgh, PA
[18] Delley B 1990 *J. Chem. Phys.* **92** 508